

**THE COMPOSITION OF AMORPHOUS PHASES IN SOILS AND SEDIMENTS ON EARTH AND MARS.** R. J. Smith<sup>1</sup>, B. Horgan<sup>1</sup>, E. Rampe<sup>2</sup> and E. Dehouck<sup>3</sup>, <sup>1</sup>Purdue University (rebecca.smith@purdue.edu), <sup>2</sup>NASA/Johnson Space Center, <sup>3</sup>LGL-TPE, Université de Lyon, France.

**Introduction:** Amorphous phases are major components (~15-70 wt%) of all rock and soil samples measured thus far by the CheMin X-ray diffractometer (XRD) instrument on the MSL rover in Gale crater, Mars [1-7]. The nature of these phases is not well understood and could be any combination of primary (e.g., glass) and secondary (e.g., silica, ferrihydrite) phases. Secondary amorphous phases are frequently found as weathering products in soils on Earth [e.g., 8-10], but these materials remain poorly characterized, and it is not certain how properties like composition and structure change with formation environment.

CheMin mineral abundances combined with bulk chemical composition from the Alpha Particle X-ray Spectrometer (APXS) have been used to estimate the composition of the XRD amorphous materials in soil and rock samples in Gale crater [2-7, 11]. Here we apply a similar approach to a diverse suite of basaltic terrestrial samples, combining bulk XRD mineralogy with bulk chemical compositions to calculate the bulk composition of the amorphous component (AmC). We also utilize transmission electron microscopy (TEM) and energy dispersive x-ray spectroscopy (EDS) to study the composition of individual amorphous phases at the nanometer scale. Bulk and individual terrestrial AmC compositions are then compared to bulk AmC compositions calculated for samples in Gale crater.

**Methods:** We apply the mass balance calculations of [11] to a suite of terrestrial samples. Our sample suite includes: sediments from recently de-glaciated volcanoes (Oregon) [12], modern volcanic soils (Hawaii) [13], and volcanic paleosols (Oregon) [14] in order to determine how formation environment, climate, and diagenesis affect the abundance and composition of amorphous phases.

Mineral abundances are derived from Rietveld refinements using JADE and HighScore+ software of XRD patterns measured on a Panalytical instrument with a Co-K $\alpha$  source. Elemental chemistry is measured via XRF, titration (FeO), IR (SO<sub>3</sub>), and INAA (Cl).

Soil and sediment samples were dried under a fume hood then sieved to <150  $\mu$ m to be consistent with CheMin measurements. Paleosols were broken down into pebble and sand-sized particulates using a rock hammer. XRD powders were prepared in a micronizing mill with internal standards (20 wt.% Al<sub>2</sub>O<sub>3</sub>) to quantify crystalline and amorphous phases. Samples for TEM were powdered in the same way, without an internal standard, and were then dispersed onto carbon coated copper grids. TEM analyses were performed using an FEI Talos F200X at Purdue.

**Results:** *Bulk amorphous component composition.* Initial calculations suggest that the AmCs consist primarily of SiO<sub>2</sub>, Al<sub>2</sub>O<sub>3</sub>, TiO<sub>2</sub>, FeO and Fe<sub>2</sub>O<sub>3</sub>, with minor amounts of other oxides (e.g., MgO, CaO, Na<sub>2</sub>O; Figure 1). Compared to their respective crystalline counterparts, calculations indicate bulk AmCs enriched in SiO<sub>2</sub> for the glacial samples, and depleted in SiO<sub>2</sub> for the modern soil and paleosol samples.

*Individual amorphous phase compositions.* Amorphous phases were identified in TEM by selected area electron diffraction (SAED) patterns exhibiting diffuse rings and no diffraction spots. The amorphous phases generally display one of three morphologies: (1) fluffy, (2) nodular, or (3) massive (Figure 2). Fluffy phases are defined as having irregular and diffuse boundaries. They are frequently associated with clay minerals or precursors and commonly have a fibrous or platy appearance.

These observations are consistent with the origin of these phases as weathering products. Nodular phases have relatively well-defined boundaries consisting of spherical shapes (~5-10 nm in diameter) that are frequently found as either a clump or a coating on top of other grains. These are most likely weathering products. Massive phases have well defined boundaries, they frequently contain crystalline phenocrysts, and could be either primary glass

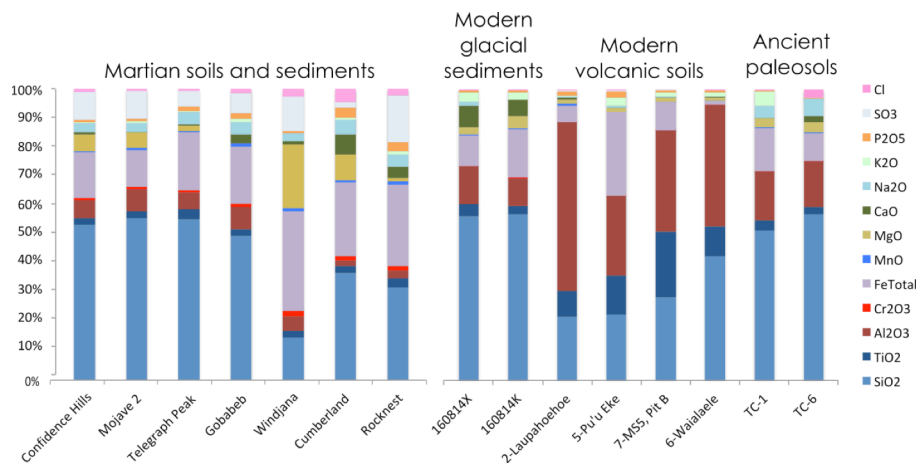
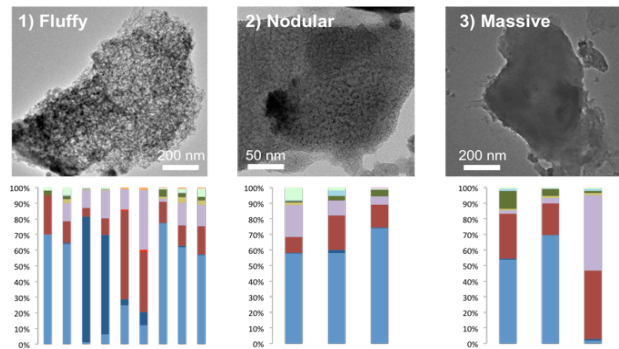


Figure 1. Bulk amorphous component compositions derived from mass balance calculations.

or secondary phases. Examples of all three morphologies can be found in most samples, and each morphology displays a range of compositions (Figure 2). The individual phases are predominantly made of  $\text{SiO}_2$ ,  $\text{Al}_2\text{O}_3$ ,  $\text{TiO}_2$ ,  $\text{FeO}_T$ , with minor amounts of other oxides (e.g.,  $\text{MgO}$ ,  $\text{CaO}$ ,  $\text{Na}_2\text{O}$ ; Figure 2), consistent with bulk compositions derived from mass balance calculations.



**Figure 2.** TEM images showing examples of the amorphous phase morphology categories described in the text (top) along with the range of EDS-measured compositions displayed by each morphology (bottom). Same legend as Figure 1.

**Discussion:** If the AmC of our samples primarily consists of weathering products, our results show that bulk amorphous compositions do vary between weathering environments – in particular, the relative enrichment or depletion in silica. Although silica is highly mobile during weathering in all mafic environments [15], colder and more rapid weathering during melt events in glacial environments preferentially forms poorly crystalline phases that take up the silica in solution [16], whereas in warmer and wetter environments, the silica is taken up by more crystalline minerals. However, more TEM work is needed to help distinguish the mass fractions of primary volcanic glass and amorphous weathering products represented in our samples.

TEM analyses reveal that the AmCs consist of several different phases. These phases have compositions with varying ratios of  $\text{SiO}_2$ ,  $\text{Al}_2\text{O}_3$ ,  $\text{TiO}_2$ , and  $\text{FeO}_T$ , many phases deviating from well-known amorphous phase compositions (e.g., allophane, ferrihydrite) and volcanic glass. These results show that many distinct amorphous weathering phases can form within a single soil environment, and that bulk amorphous abundances should not be expected to match the composition of a single amorphous phase.

**Comparison to martian samples:** It is important to note a few limitations of the mass balance calculation method before comparing terrestrial to martian AmC compositions. First, the composition of crystalline phases that are below the detection limit of XRD

will, be allocated to the AmC composition. Second, minor elemental substitutions not reported in the ideal structure formula for crystalline minerals are not reflected in the XRD models, and so they are also allocated to the AmC composition. Third, clay minerals can have complex compositions, and when poorly constrained, their presence makes it difficult to precisely determine the AmC compositions [11]. With these caveats in mind, we can start to make some general comparisons.

Like our glacier samples, the Confidence Hills (CH), Mojave 2 (MJ), Telegraph Peak (TP), and Gobabeb (GB) martian samples all have bulk AmCs with elevated  $\text{SiO}_2$  compared to their crystalline components [6-7]. Additionally, the overall bulk AmC compositions of these martian samples are most similar to our glacial sediment samples, with the exception of higher  $\text{SO}_3$  and  $\text{Cr}_2\text{O}_3$  in the martian samples (Figure 1). The high  $\text{SO}_3$  abundances in CH, MJ, and TP rock samples has been attributed to episodes of diagenesis [e.g., 6 and references within], whereas the high  $\text{SO}_3$  in the GB sand sample is most likely due to dust [7].

The Windjana, Cumberland, and Rocknest martian samples exhibit a markedly different bulk amorphous composition compared to our terrestrial samples, with depleted silica along with low  $\text{Al}_2\text{O}_3$  abundances and higher abundances of mono- and divalent cation oxides (e.g.,  $\text{MgO}$ ,  $\text{Na}_2\text{O}$ ) than any bulk or individual amorphous composition observed in our samples thus far. Rocknest is a dusty sample, so this suggests that martian dust has a very different amorphous composition compared to typical terrestrial weathering products.

Lastly, it should be noted that some of the compositional differences between terrestrial and martian samples could be attributed to differences in starting material composition. More work on comparing the crystalline components to the AmCs could potentially help explain some of these differences.

**References:** [1] Bish et al. (2013) *Science*, 341. [2] Blake et al. (2013) *Science*, 341. [3] Vaniman et al. (2014) *Science*, 343. [4] Morris et al. (2016) *PNAS*, 113, 7071-7076. [5] Treiman et al. (2016) *JGR: Planets*, 121, 75–106. [6] Rampe et al. (2017) *EPSL*, 471, 172-185. [7] Achilles et al. (2017) *JGR: Planets*, 122, 2344–2361. [8] Colman (1982) *Geo. Survey Prof. Paper 1246*. [9] Wada (1987) *Chem. Geo.*, 60, 17-28. [10] Fedotov et al. (2006) *Eur. Soil Sci.*, 39, 738-747. [11] Dehouck et al. (2014) *JGR*, 119, 2640-2657. [12] Scudder et al. (2016) *47<sup>th</sup> LPSC*, 2937. [13] Retallack et al. (1999) *Geo. Soc. Am.*, 344. [14] Ziegler et al. (2003) *Chem. Geo.*, 202, 461–478. [15] McLennan et al. (2003) *Geo.*, 31(4), 315-318. [16] Rutledge et al (2017) *Early Mars 4*, #3070.